Supporting Information

Highly Efficient Visible-Light-Driven Oxygen-Vacancy-Based Cu$_{2+1}$O Micromotors with Biocompatible Fuels

Qinglong Wang, [‖] Renfeng Dong, [‖]* Qianxian Yang, Jiajia Wang*, Shuyu Xu, Yuepeng Cai*

School of Chemistry and Environment, Guangzhou Key Laboratory of Materials for Energy Conversion and Storage, Guangdong Provincial Engineering Technology Research Center for Materials for Energy Conversion and Storage, South China Normal University, Guangzhou, 510006, China

[‖]Qinglong Wang and Renfeng Dong contributed equally.

*Corresponding author:
Renfeng Dong: rfdong@m.scnu.edu.cn
Jiajia Wang: jjwang@m.scnu.edu.cn
Yuepeng Cai: caiyp@scnu.edu.cn

Video S1: The motion of Cu$_2$O and Cu$_{2+1}$O micromotors under blue light in pure water

Video S2: The motion of Cu$_{2+1}$O micromotors under different light (blue, green, red) intensity in pure water

Video S3: The motion of Cu$_2$O particles and Cu$_{2+1}$O micromotors in 0.2 mM tannic acid under 48.8 mW cm^{-2} blue light

Video S4: The motion of Cu$_{2+1}$O micromotors under 48.8 mW cm^{-2} blue, 235.8 mW cm^{-2} green, 83.8 mW cm^{-2} red light in different tannic acid concentration

Video S5: The motion of Cu$_{2+1}$O micromotors under different light (blue, green, red) intensity in 0.2 mM tannic acid

Video S6: The motion of the Cu$_{2+1}$O micromotor under different light in 0.05 mM tannic acid

METHODS

Synthesis of Cu$_{2+1}$O micromotor. 0.2 g copper acetate (Aladdin #C105398) and 0.03 g sodium chloride (Aladdin #I1829090) was added into a round bottom flask with 8 ml water, followed by addition of 8 ml of ethanol. In the oil bath, when the temperature reached 75 °C, 0.40 g of sodium hydroxide (Tianjin ZhiYuan Reagent Co, Ltd) were added, after 2 minutes, followed by adding 0.25 g of glucose (RichJoint Chemical), the reaction was carried out for 30 minutes with low stirring speed. The resulting dark brown precipitate was washed with DI water (18.2 MΩ cm) for 5 times, and dried at 60 °C in vacuum. Finally, Cu$_{2+1}$O micromotor (diameter: about 1 μm) were obtained. And the preparation of Cu$_2$O is based on previously reported methods.[1]

Electrochemical Measurements. The current-time curve of Cu$_{2+1}$O micromotor and Cu$_2$O particles with and without illumination in 0.5 M Na$_2$CO$_3$ is tested by electrochemical workstation CHI660E. The Cu$_{2+1}$O and Cu$_2$O samples were coated on ITO glass (length 1.0 cm and width 1.0 cm) and used as the working electrode for the electrochemical measurements. Current-time measurement was performed at a base potential of 0 V and blue light on/off at 5 s intervals (vs Ag/AgCl, 3 M KCl reference, the light intensity is 13.0 mW cm^{-2}).

Motion calibration experiments. To determine the relationship between the active motion of Cu$_{2+1}$O micromotor and light, we used the ND Filter in the microscope (4 X, 8 X, 16 X) to control the illumination intensity. The wavelength of light ranges from 450~750 nm. In this system, videos were all recorded with the 40X objective and the number of samples per experiment was 30. The average velocity was calculated and the entire procedure was repeated six times. The trajectories of each individual

particle were tracked by using the NIS-Elements AR 4.3 software. A typical video is captured with 25 frames per second. The propulsion calibration experiments were performed by mixing 2 µL of the motors dispersed in deionized water.

Equipments. XRD patterns were obtained by X-Ray Diffractomer (Bruker D8 Advance, Germany), SEM patterns were obtained by Tescan MAIA 3. The UV-vis DRS was obtained by Japan Shimadzu UV-2700 UV-Vis Spectrophotometer (with integrating sphere). The electron paramagnetic resonance (EPR) spectra measurement was carried out using an Endorspectrometer (JES FA200, Japan) at room temperature. Electrochemical workstation (CHI660E, China) was used to acquire the current-time curve. The light was generated by Mercury lamp sockets and dichroic mirror DM 400. Barrier filter BA520 was used to generate multi-spectral light, and illumination intensities were controlled by ND filters (4×, 8×, 16×) (all from Nikon). Videos were captured by an inverted optical microscope (Nikon Instrument Inc. Ti-S/L100), coupled with 40× objectives, and a Hamamatsu ORCA-flash 4.0 LT (C11440) sCMOS digital camera using the NIS-Elements AR 4.3 software. All the illumination intensities were calculated by the solar power meter (SM206-SOLAR, Xin Bao Ke Yi Inc. Shenzhen,

Figure S1. (a)(b) are the SEM image and XRD pattern of Cu_2O sample. Scale bar: 2 µm.
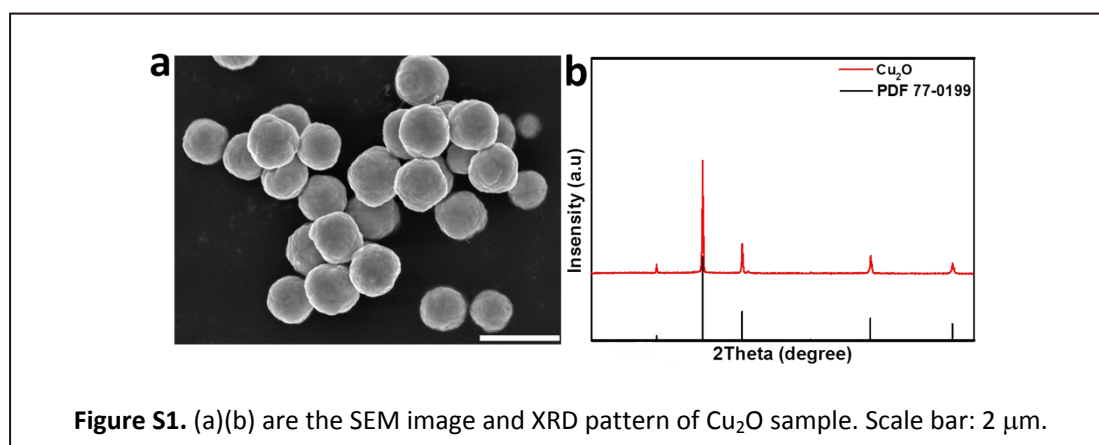
China).

We characterized the Cu_2O particles by scanning electron microscopy (SEM), X-ray diffraction (XRD) in detail. The SEM image shows the size of the motor with about 1 μm (Figure S1a), which is similar to the $Cu_{2+1}O$. XRD measurement was performed to confirm the composition of prepared samples as shown in Figure S1b, and the XRD pattern of $Cu_{2+1}O$ could be completely matched with the standard spectrum of PDF 77-0199, which shows that the sample is highly crystalline Cu_2O. It is worth noting that the XRD pattern of $Cu_{2+1}O$ shows the significant overall left shift compared to Cu_2O due to the presence of oxygen vacancies.
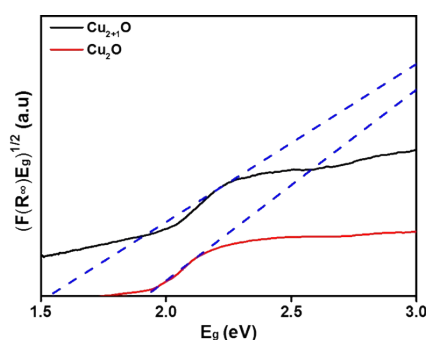

Figure S2. Band gap energy of $Cu_{2+1}O$ and Cu_2O.

According to Figure S1, the band gap energy of $Cu_{2+1}O$ and Cu_2O were 1.54 eV, 1.93 eV respectively. It suggested that the light-active ability of Cu_2O improved in the existence of oxygen vacancy. This is due to oxygen vacancy can generate impurity energy levels and mixed valence states in the band gap of Cu_2O. These changes decrease the energy band gap, which is in agreement with the calculated results.
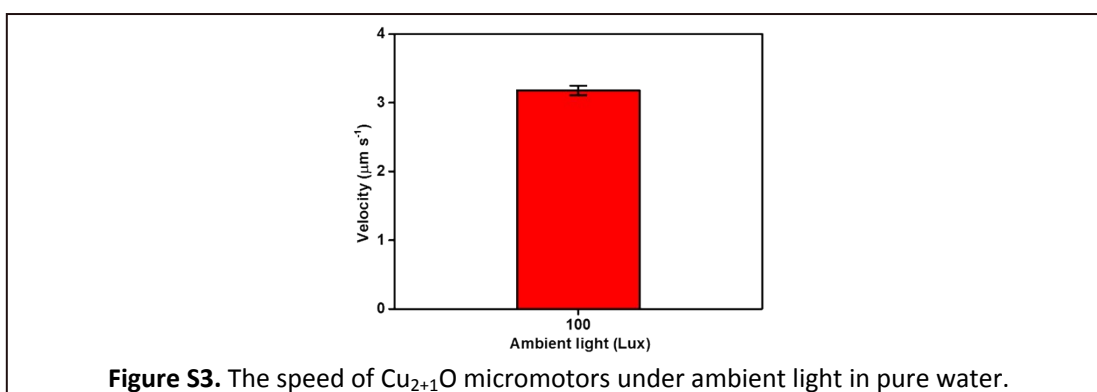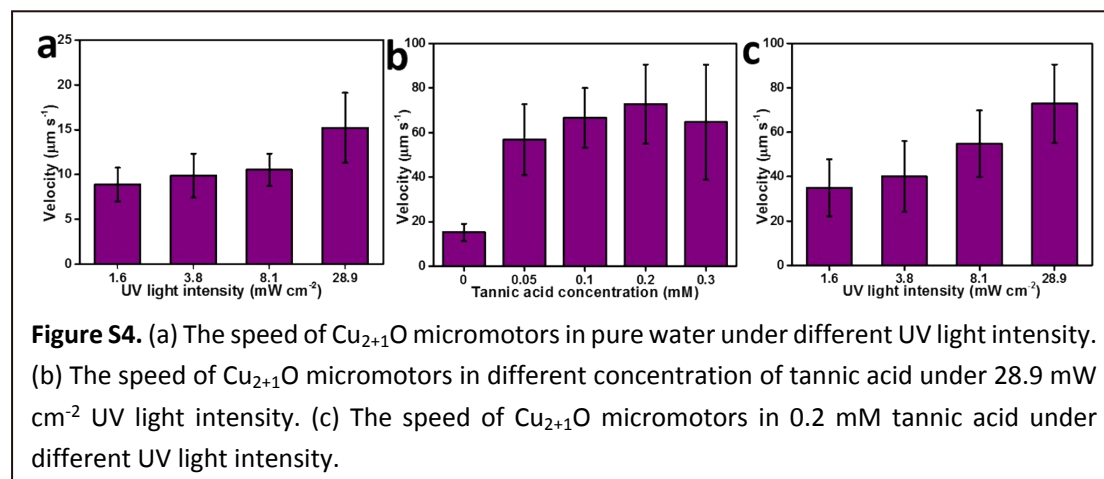

Figure S3. The speed of $Cu_{2+1}O$ micromotors under ambient light in pure water.

We also confirmed the speed of the $Cu_{2+1}O$ micromotors under ambient light in pure water, which was only 3.18 μm s^{-1}, and the $Cu_{2+1}O$ micromotors merely exhibit Brownian motion.

Figure S4. (a) The speed of $Cu_{2+1}O$ micromotors in pure water under different UV light intensity. (b) The speed of $Cu_{2+1}O$ micromotors in different concentration of tannic acid under 28.9 mW cm^{-2} UV light intensity. (c) The speed of $Cu_{2+1}O$ micromotors in 0.2 mM tannic acid under different UV light intensity.

We have further confirmed the speeds of $Cu_{2+1}O$ micromotors under UV light. The $Cu_{2+1}O$ micromotors show excellent performance both in pure water and low concentration tannic acid under UV light, it is worth mentioning that the best propulsion performance of such motors is still under blue light. Figure S4a illustrates the speed of the $Cu_{2+1}O$ micromotors in pure water under different UV light intensity. With the light intensity increases, the motor speed also increases, and the speed increase from 8.87 to 15.22 μm s^{-1} under 1.6 and 28.9 mW cm^{-2} UV light intensity respectively. While, in 0.05 mM tannic acid, $Cu_{2+1}O$ micromotors exhibit dramatic speed acceleration of 56.76 μm s^{-2}, which about 3.7 times in pure water (Figure S4b). Further, Figure S4c shows the relationship between motors speed and UV light intensity under 0.2 mM tannic acid, and those motors reach the maximum speed at 72.80 μm s^{-1} under 28.9 mW cm^{-2} UV light.

Table S1. Comparison of different visible-light-driven micromotors

Motor	Visible Light wavelength	Light intensity	Fuel concentration	Max speed	Ref.
Cu_2O-Au Janus micromotors	>380 nm	1360 mW/cm^2	3v% H_2O_2	6 μm/s	1
$BiVO_4$ micromotors	>380 nm	2500 mW/cm^2	0.1wt% H_2O_2	≈5 μm/s	2
Si nanowire	500~800 nm	100 mW/cm^2	0.5wt% H_2O_2	≈37.5 μm/s	3

TPM- Fe_2O_3	430~490 nm	/	3wt% H_2O_2	15 μm/s	4
Au–Fe_2O_3 nanowire	>380 nm	3000 mW/cm^2	2.5V.% H_2O_2	≈30 μm/s	5
Au/B-TiO_2 micromotor	420~440 nm	1800 mW/cm^2	3wt% H_2O_2	≈9 μm/s	6
Fe_2O_3 nanomotor (Hematite)	430~490 nm	/	1wt%H_2O_2, and highly basic pH	4.5 μm/s	7
$Zn_{0.7}Cd_{0.3}$Se-Cu_2Se-Pt nanowire	550 nm	250 mW/cm^2	20 mM QH$_2$ and 1 mM BQ	≈11 μm/s	8
TiO_2-Si nanotree	~660 nm	328 mW/cm^2	100 mM QH$_2$ and 1 mM BQ	≈8.7 μm/s	9
Cu_2O@N-CNTs micromotor	510~560 nm	55300 Lux	30 mM glucose	18.71 μm/s	10
SOM-based nanomotor	510~590 nm	30000 lux	H_2O	≈10 μm/s	11
Si–Au micromotors	>380 nm	1360 mW/cm^2	H_2O	≈5 μm/s	12
BiOI-Au Janus micromotor	450~560	43900 Lux	H_2O	1.6 μm/s	13
$Cu_{2+1}O$ micromotor	450~490 nm	48.8 mW/cm^2	H_2O	18.10 μm/s	This work
	450~490 nm	48.8 mW/cm^2	0.2 mM tannic acid	107.32 μm/s	This work

References

1　　D. Zhou, Y.C. Li, P. Xu, N.S. McCool, L. Li, W. Wang, T.E. Mallouk, *Nanoscale* **2017**, *9*, 75.

2　　K. Villa, F. Novotný, J. Zelenka, M.P. Browne, T. Ruml, M. Pumera, *ACS Nano* **2019**, *13,* 8135.

3　　J. Wang, Z. Xiong, X. Zhan, B. Dai, J. Zheng, J. Liu, J. Tang, *Adv. Mater.* **2017**, *29*, 1701451.

4　　J. Palacci, S. Sacanna, A.P. Steinberg, D.J. Pine, P.M. Chaikin, *Science* **2013**, *339*, 936.

5　　D. Zhou, L. Ren, Y.C. Li, P. Xu, Y. Gao, G. Zhang, W. Wang, T.E. Mallouk, L. Li, *Chem. Commun.* **2017**, *53*, 11465.

6　　B. Jang, A. Hong, H.E. Kang, C. Alcantara, S. Charreyron, F. Mushtaq, E. Pellicer, R. Büchel, J. Sort, S.S. Lee, B.J. Nelson, S. Pané, *ACS Nano* **2017**, *11*, 6146.

7　　J. Palacci, S. Sacanna, A. Vatchinsky, P.M. Chaikin, D.J. Pine, *J. Am. Chem. Soc.* **2013**, *135*, 15978.

8　　J. Zheng, J. Wang, Z. Xiong, Z. Wan, X. Zhan, S. Yang, J. Chen, J. Dai, J. Tang, *Adv. Funct. Mater.* **2019**, *29*, 1901768.

9　　J. Zheng, B. Dai, J. Wang, Z. Xiong, Y. Yang, J. Liu, X. Zhan, Z. Wan, J. Tang, *Nat. Commun.* **2017**, *8*, 1438.

10　　Q. Wang, R. Dong, C. Wang, S. Xu, D. Chen, Y. Liang, B. Ren, W. Gao, Y. Cai, *ACS Appl. Mater. Inter.* **2019**, *11*, 6201.

11　　A. Mallick, S. Roy, *Nanoscale* **2018**, *10*, 12713.

12　　D. Zhou, Y.C. Li, P. Xu, L. Ren, G. Zhang, T.E. Mallouk, L. Li, *Nanoscale* **2017**, *9,* 11434.

13   R. Dong, Y. Hu, Y. Wu, W. Gao, B. Ren, Q. Wang, Y. Cai, *J. Am. Chem. Soc.* **2017**, *139*, 1722.